

NONLINEAR FEEDFORWARD AND FEEDBACK TRACKING CONTROL WITH INPUT CONSTRAINTS SOLVING THE PENDUBOT SWING-UP PROBLEM

Knut Graichen Michael Zeitz

*Institut für Systemdynamik und Regelungstechnik,
Universität Stuttgart, Germany
{graichen,zeitz}@isr.uni-stuttgart.de*

Abstract: The swing-up maneuver of a pendubot is achieved by a tracking control with separate design of a nonlinear feedforward and a linear feedback part. The inversion-based feedforward control treats the swing-up as a two-point boundary value problem with input constraints in the coordinates of the input-output normal form and is numerically calculated by a standard MATLAB solver. The feedback part with time-variant gains is designed as an LQR controller for the pendubot model linearized along the nominal trajectories. The tracking control is validated in experimental swing-up maneuvers of the pendubot. *Copyright© 2005 IFAC*

Keywords: Two-degree-of-freedom control, nonlinear system inversion, internal dynamics, non-minimum phase, boundary value problem

1. INTRODUCTION

The pendubot is a two-link planar robot arm with an actuator at the shoulder and none at the elbow, which is widely used in nonlinear control education and research due to challenging features like unstable internal dynamics, nonholonomic behavior, and the lack of feedback linearizability. A particularly difficult control task is swinging up the pendubot from its stable downward equilibrium position to the unstable upward equilibrium position.

The swing-up problem has been studied by several authors. Spong and Block (1995) used a partial feedback linearization technique for the swing-up maneuver, and a linear controller stabilizes the pendubot in the upward position, see (Spong, 1995) for further information. In (Fantoni *et al.*, 2000), a control strategy based on energy considerations is studied on the basis of simulation results. A further swing-up technique presented by Absil and Sepulchre (2001) appropriately switches between equilibrium points of the actuator in order to pump energy into the system.

In this paper, the swing-up maneuver is addressed in order to illustrate the nonlinear inversion-based feedforward design technique proposed by the authors (Graichen *et al.*, 2004a; Graichen *et al.*, 2004b) as part of the two-degree-of-freedom control scheme illustrated in Figure 1. The inversion-based feedforward control Σ_{FF} solves the swing-up maneuver of the pendubot Σ as a two-point boundary value problem (BVP) defined on a finite-time interval by employing the standard MATLAB function `bvp4c` (Shampine *et al.*, 2000). This approach is further elaborated by considering input constraints for the resulting feedforward control trajectory $u^*(t)$.

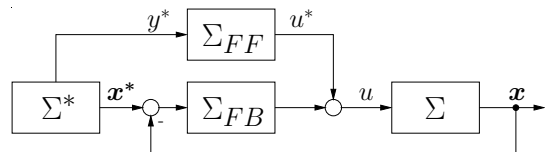


Fig. 1. Two-degree-of-freedom control scheme with system Σ , feedback control Σ_{FB} , feedforward control Σ_{FF} , and signal generator Σ^* .

The state feedback control Σ_{FB} is required for the stabilization of the swing-up maneuver. Due to the accuracy of the nonlinear feedforward control, Σ_{FB} can be designed by linear methods with the pendubot model linearized along the nominal state trajectories $\mathbf{x}^*(t)$, which are provided by the signal generator Σ^* . An experimental swing-up maneuver of the pendubot is used to illustrate the performance of the tracking control.

2. SWING-UP MANEUVER OF THE PENDUBOT

The considered pendubot consists of an inner arm with the angle $\phi(t)$, which is connected to an actuator with the constrained torque $|u(t)| \leq u_{max}$, and an outer arm moving freely around the joint M with the angle $\psi(t)$, see Figure 2. Detailed investigations on the pendubot and the similar acrobot (with the actuator at the elbow joint M) can be found in (Murray and Hauser, 1990; Spong, 1995; Block and Spong, 1995).

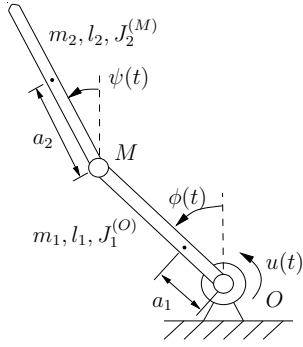


Fig. 2. Scheme of the pendubot with the angles $\phi(t)$, $\psi(t)$, the input $u(t)$, and the respective mechanical parameters in Table 1.

The equations of motion are given by

$$A \ddot{\phi} + B \ddot{\psi} + C = u(t), \quad (1)$$

$$D \ddot{\phi} + E \ddot{\psi} + F = 0 \quad (2)$$

with

$$\begin{aligned} A &= (J_1^{(O)} + m_2 l_1^2), & B &= m_2 l_1 a_2 \cos(\phi - \psi), \\ C &= m_2 l_1 a_2 \dot{\psi}^2 \sin(\phi - \psi) - (m_1 g a_1 + m_2 g l_1) \sin \phi, \\ D &= m_2 l_1 a_2 \cos(\phi - \psi), & E &= J_2^{(M)}, \\ F &= -m_2 l_1 a_2 \dot{\phi}^2 \sin(\phi - \psi) - m_2 g a_2 \sin \psi. \end{aligned}$$

Table 1. Parameters of the pendubot.

Parameter	Value	Parameter	Value
$J_1^{(O)}$	0.0455 kg m ²	$l_1 = l_2$	0.45 m
$J_2^{(M)}$	0.0076 kg m ²	m_2	0.11 kg
$m_1 g a_1$	0.433 Nm	a_2	0.21 m

The swing-up maneuver of the pendubot within a finite-time interval $t \in [0, T]$ means the transition

from its stable downward equilibrium $\phi(0) = \psi(0) = -\pi$ to its unstable upward equilibrium $\phi(T) = \psi(T) = 0$ with $\phi^{(i)}|_{0,T} = \psi^{(i)}|_{0,T} = 0$, $i = 1, 2$.

With respect to the two-degree-of-freedom control scheme in Figure 1, the feedforward control Σ_{FF} has to provide a nominal input trajectory $u^*(t)$ which steers the pendubot from the downward equilibrium to the upward equilibrium within the time $t \in [0, T]$. Since the actual constraints of the actuator are $|u(t)| \leq u_{max} = 1$ Nm, the nominal input trajectory is specified to $|u^*(t)| \leq \hat{u} = 0.7$ Nm, in order to leave sufficient torque reserve for the underlying feedback control Σ_{FB} which stabilizes the pendubot along the nominal trajectories, see Figure 1.

2.1 Nonlinear input-output normal form

The inversion-based feedforward control $u^*(t)$, $t \in [0, T]$ of the swing-up maneuver is designed in the input-output normal form coordinates of the pendubot model (1)–(2), cf. (Graichen *et al.*, 2004a; Graichen *et al.*, 2004b). By choosing the angle of the inner arm as the output $y = \phi$, the system (1)–(2) has the relative degree $r = 2$. With the coordinates $(y, \eta) = (\phi, \psi)$, the nonlinear input-output normal form (Isidori, 1995)

$$\ddot{y} = \frac{E}{G} \left(\frac{BF}{E} - C + u(t) \right) = \alpha(y, \dot{y}, \eta, \dot{\eta}, u), \quad (3)$$

$$\ddot{\eta} = \frac{D}{G} \left(-\frac{AF}{D} + C - u(t) \right) = \beta(\eta, \dot{\eta}, y, \dot{y}, u) \quad (4)$$

with $G = AE - BD$ comprises the input-output dynamics (3) and the internal dynamics (4).¹ An intrinsic feature of the pendubot is that the zero dynamics associated to (4) is stable for the downward equilibrium position $y = \eta = -\pi$, and is unstable for the upward equilibrium position $y = \eta = 0$, i.e. both minimum phase and non-minimum phase behavior occur.

The swing-up of the pendubot within the finite-time interval $t \in [0, T]$ means that the solutions of the ODEs (3)–(4) have to satisfy the boundary conditions (BCs)

$$y(0) = -\pi, \quad y(T) = 0, \quad \dot{y}|_{0,T} = 0, \quad (5)$$

$$\eta(0) = -\pi, \quad \eta(T) = 0, \quad \dot{\eta}|_{0,T} = 0. \quad (6)$$

From a mathematical point of view, the two second order ODEs (3)–(4) and the eight BCs (5)–(6) form two coupled nonlinear two-point BVPs for $y(t)$ and $\eta(t)$. The solutions $y(t)$ and $\eta(t)$ defined on $t \in [0, T]$ essentially depend on the swing-up time T and the constrained input trajectory $|u(t)| \leq \hat{u}$.

¹ With the parameters in Table 1, $G = AE - BD > 0$ holds, and the relative degree $r = 2$ is well-defined due to $E \neq 0$.

2.2 Swing-up time and time scaling

The swing-up time T is an intrinsic property of the swing-up problem, which has to be determined appropriately in course of the feedforward control design. This instance can be illustrated by considering the equilibria (ϕ_s, ψ_s) with $\phi_s^{(i)} = \psi_s^{(i)} = 0$, $i = 1, 2$ in dependence of the stationary input u_s . In view of the pendubot model (1)–(2), the following sets of equilibria

$$S_k = \left\{ (\phi_s, \psi_s) \in \mathbb{R}^2 : (\phi_s, \psi_s) = \left(\arcsin \frac{u_s}{m_2 g l_1 + m_1 g a_1}, k \pi \right), u_s \in \mathbb{R} \right\}, k \in \mathcal{N}^0$$

are derived. Thereby, the downward equilibrium $(\phi_s, \psi_s) = (-\pi, -\pi) \in S_{-1}$ and the upward equilibrium $(\phi_s, \psi_s) = (0, 0) \in S_0$ lie in two non-connected sets, and therefore no stationary connection exists between the lower and the upper equilibrium. This directly associates that the swing-up of the pendubot is not possible arbitrarily slowly with a corresponding long transition time T .

Furthermore, the consideration of input constraints $|u^*(t)| \leq \hat{u}$, $t \in [0, T]$ for the feedforward control will result in a modified swing-up time T with respect to a swing-up time T_0 in the unconstrained case. This instance is taken into account by introducing the time transformation

$$t = \epsilon \tau, \quad T = \epsilon T_0 \quad (7)$$

with the new time coordinate $\tau \in [0, T_0]$. The scaling factor ϵ denotes the variation of the swing-up time T with respect to T_0 in the unconstrained case, which has to be reasonably determined.

By applying the time scaling (7) to the input-output normal form (3)–(4), the right-hand sides become $\alpha_\epsilon(y, y', \eta, \eta', u, \epsilon) := \alpha(y, y'/\epsilon, \eta, \eta'/\epsilon, u)$ and $\beta_\epsilon(\eta, \eta', y, y', u, \epsilon) := \beta(\eta, \eta'/\epsilon, y, y'/\epsilon, u)$ with $(\cdot)' = d/d\tau$.² Then, the input-output dynamics (3) and the internal dynamics (4) can be expressed in the new time coordinate $\tau \in [0, T_0]$ with

$$y'' = \epsilon^2 \alpha_\epsilon(y, y', \eta, \eta', u, \epsilon), \quad (8)$$

$$\eta'' = \epsilon^2 \beta_\epsilon(\eta, \eta', y, y', u, \epsilon) \quad (9)$$

subject to the eight BCs

$$y(0) = -\pi, \quad y(T_0) = 0, \quad y'|_{0, T_0} = 0, \quad (10)$$

$$\eta(0) = -\pi, \quad \eta(T_0) = 0, \quad \eta'|_{0, T_0} = 0, \quad (11)$$

which directly follow from (5)–(6). The two coupled nonlinear two-point BVPs (8)–(9) with (10)–(11) are defined on the fixed time interval $\tau \in [0, T_0]$, in contrast to the original BVPs (3)–(6). The solutions $y(\tau)$ and $\eta(\tau)$ depend on the scaling factor ϵ and the constrained input trajectory $|u(\tau)| \leq \hat{u}$. The determination of $y(\tau)$, $\eta(\tau)$, ϵ ,

and $u^*(\tau)$ is the main objective of the feedforward control design in the next section.

3. FEEDFORWARD CONTROL DESIGN

The inversion-based design of the nonlinear feedforward control is based on the inverse input-output dynamics (8)

$$u^*(\tau) = \alpha_\epsilon^{-1}(y^*, y^{*'}, y^{*''}/\epsilon^2, \eta^*, \eta^{*'}, \epsilon), \quad (12)$$

which enables an explicit calculation of the input trajectory $u^*(\tau)$ in dependence of the output $y^*(\tau)$, the internal dynamics state $\eta^*(\tau)$, and the scaling factor ϵ . This concept is an elaboration of (Graichen *et al.*, 2004a; Graichen *et al.*, 2004b), where the feedforward control design is introduced for a fixed transition time T in the original time coordinate $t \in [0, T]$ without the consideration of input constraints.

3.1 BVPs for constrained input

In order to determine the trajectories $y^*(\tau)$ and $\eta^*(\tau)$, the BVPs (8)–(11) are rewritten in an appropriate manner by placing the feedforward control (12) into the internal dynamics (9). Moreover, a new function $\hat{\alpha} = y^{*''}/\epsilon^2$ for the second time derivative $y^{*''}$ of the output yields the two associated second-order BVPs

$$y^{*''} = \epsilon^2 \hat{\alpha}, \quad (13)$$

$$\eta^{*''} = \epsilon^2 \bar{\beta}_\epsilon(\eta^*, y^*, y^{*'}, \hat{\alpha}, \epsilon) \quad (14)$$

with $\bar{\beta}_\epsilon(\cdot) = -(D\hat{\alpha} + F)/E$ and the eight BCs

$$y^*(0) = -\pi, \quad y^*(T_0) = 0, \quad y^{*'}|_{0, T_0} = 0, \quad (15)$$

$$\eta^*(0) = -\pi, \quad \eta^*(T_0) = 0, \quad \eta^{*'}|_{0, T_0} = 0. \quad (16)$$

Note that the representations (12)–(16) are equivalent to the previous BVPs (8)–(11). The solutions $y^*(\tau)$ and $\eta^*(\tau)$ of the BVPs (13)–(16) and the feedforward trajectory $u^*(\tau)$ in (12) mainly depend on the set-up of the function $\hat{\alpha} = y^{*''}/\epsilon^2$ with respect to the following objectives:

- (i) \mathcal{C}^0 -continuity of the feedforward trajectory $u^*(\tau)$ at the bounds $\tau = 0, T_0$ implies that the output trajectory $y^*(\tau)$ must meet the two additional BCs

$$y^{*''}(0) = 0, \quad y^{*''}(T_0) = 0. \quad (17)$$

- (ii) The solvability of the BVPs (13)–(16), defined by two second order ODEs and eight BCs, requires at least three free parameters besides the scaling factor ϵ . In the design approach (Graichen *et al.*, 2004a; Graichen *et al.*, 2004b), the parameters $\mathbf{p}^* = (p_1^*, p_2^*, p_3^*)$ are provided in a set-up function

² To simplify matters, the symbols y , η , and u represent the same quantities in both time coordinates t and τ .

$\Upsilon(\tau, T_0, \mathbf{p}^*)$, $\tau \in [0, T_0]$ for the output $y^*(\tau)$, which is constructed by the cosine series³

$$\Upsilon(\tau, T_0, \mathbf{p}^*) = \sum_{i=0}^3 a_i(\mathbf{p}^*) \cos \frac{i\pi\tau}{T_0} + \sum_{i=1}^3 p_i^* \cos \frac{(i+3)\pi\tau}{T_0}. \quad (18)$$

The free parameters p_i^* , $i = 1, 2, 3$ are the coefficients of the highest frequencies and the coefficients $a_i(\mathbf{p}^*)$, $i = 0, 1, 2, 3$ depend on the parameters \mathbf{p}^* such that the six BCs for $y^*(\tau)$ in (15) and (17) are satisfied. If no input constraints are given, the second time derivative of the set-up (18) yields $\hat{\alpha} = \Upsilon''(\tau, T_0, \mathbf{p}^*)$ in (13) and (14).

- (iii) The consideration of constraints $|u^*(t)| \leq \hat{u}$ requires to check if the input

$$u_{\Upsilon} = \alpha_{\epsilon}^{-1}(y^*, y^{*'}, \Upsilon''(\tau, T_0, \mathbf{p}^*), \eta^*, \eta^{*'}, \epsilon)$$

which results if $\hat{\alpha} = \Upsilon''(\tau, T_0, \mathbf{p}^*)$ is used in (12), lies within the specified bounds. If u_{Υ} is outside the bounds, $\hat{\alpha}$ must be “re-planned” in (13)–(14), such that the bounds $\pm\hat{u}$ are met. This is accomplished by the following case-dependent definition of the function

$$\hat{\alpha} = \begin{cases} \Upsilon''(\tau, T_0, \mathbf{p}^*) & \text{if } |u_{\Upsilon}| < \hat{u} \\ \alpha_{\epsilon}(y^*, y^{*'}, \eta^*, \eta^{*'}, -\hat{u}, \epsilon) & \text{if } u_{\Upsilon} \leq -\hat{u} \\ \alpha_{\epsilon}(y^*, y^{*'}, \eta^*, \eta^{*'}, \hat{u}, \epsilon) & \text{if } u_{\Upsilon} \geq \hat{u}. \end{cases} \quad (19)$$

The calculation of the feedforward control $u^*(\tau)$, $t \in [0, T_0]$ in (12) for the swing-up maneuver requires the solution of the BVPs (13)–(16) with (18)–(19) in dependence of the free parameters ϵ and \mathbf{p}^* . Thereby, the two additional BCs in (17) are already satisfied by the set-up function $\Upsilon(\tau, T_0, \mathbf{p}^*)$ in (18), and $\hat{\alpha} = \Upsilon''(\tau, T_0, \mathbf{p}^*)$ for $\tau = 0, T_0$ in (19) holds because $u_{\Upsilon} = 0 < \hat{u}$ is the stationary input at the bounds $\tau = 0, T_0$ for the downward and the upward equilibrium.

In the special case that the feedforward control $|u^*(\tau)| < \hat{u}$ lies within the bounds for the whole transition interval $\tau \in [0, T_0]$, $y^{*''}(\tau) = \epsilon^2 \Upsilon''(\tau, T_0, \mathbf{p}^*)$ leads to $y^*(\tau) = \epsilon^2 \Upsilon(\tau, T_0, \mathbf{p}^*)$. Thereby, $\epsilon = 1$ holds, since the set-up function $\Upsilon(\tau, T_0, \mathbf{p}^*)$ in (18) already satisfies the six BCs (15) and (17). This directly corresponds to the unconstrained case with the swing-up time $T = T_0$, and the output trajectory $y^*(\tau) = \Upsilon(\tau, T_0, \mathbf{p}^*)$ is exactly the planned trajectory (18). This means that only the second-order BVP (14) of the internal dynamics has to be solved, which requires only two free parameters p_1^*, p_2^* in the set-up (18) of the output trajectory $y^*(t)$, cf. (Graichen *et al.*, 2004a; Graichen *et al.*, 2004b).

3.2 Numerical solution of the BVPs

The nonlinear BVPs (13)–(16) with (18)–(19) including four unknown parameters ϵ and $\mathbf{p}^* = (p_1^*, p_2^*, p_3^*)$ can be solved with the standard MATLAB function `bvp4c` (Shampine *et al.*, 2000). The `bvp4c`-function is a finite-difference code and determines a numerical solution by solving a system of algebraic equations resulting from the difference approximation. Moreover, `bvp4c` estimates the error of the numerical solution on each subinterval and adapts the mesh points. The user must provide the initial points of the mesh as well as a guess of the solution at the mesh points. Furthermore, an initial guess of the free parameters of the BVP is needed.

A linear interpolation between the respective BCs on a uniform mesh with 50 grid points $\tau_k \in [0, T_0]$ serves as a reasonable guess for the trajectory $\eta^*(\tau_k)$. The initial guesses of the unknown parameters are $\mathbf{p}^* = \mathbf{0}$ and $\epsilon = 1$, respectively. Then, the set-up function $\Upsilon(\tau_k, T_0, \mathbf{0})$ provides the initial profile for the output trajectory $y^*(\tau_k)$.

The solution of the BVPs (13)–(16) with (18)–(19) is highly sensitive with respect to the input constraints \hat{u} and the swing-up time T_0 in the unconstrained case. In a first step, the unconstrained case with $\hat{u} \rightarrow \infty$ is considered, and the BVPs (13)–(16) with (18)–(19) are iteratively solved in order to appropriately determine the swing-up time $T_0 = 3.5$ s. Thereby, the resulting feedforward control $|u^*(\tau)| < 1.4$ Nm violates the specified constraints of $\hat{u} = 0.7$ Nm.

In the next step, the input constraints $|u^*(\tau)| \leq \hat{u}$ are considered by solving the BVPs (13)–(16) with (18)–(19) in three successive runs of the MATLAB BVP-solver `bvp4c`. This iterative procedure is necessary due to the high sensitivity of the feedforward control with respect to \hat{u} , whereby the two last runs with decreasing input constraints use the final profiles and free parameters of the preceding run as initial guesses. For the input constraints $\hat{u} = 0.7$ Nm, this leads to the scaling factor $\epsilon = 1.475$ and the swing-up time $T = \epsilon T_0 = 5.16$ s.

Figure 3 shows the computed trajectories of $y^*(t)$, $\eta^*(t)$, and $u^*(t)$ in the real time coordinate $t = \epsilon\tau$, as well as time-discrete snapshots of the pendubot to illustrate the counter-clockwise swing-up maneuver. The parameterizing function $\hat{\alpha}$ in (19) is illustrated in Figure 4, where the second derivative of the output $\ddot{y}^*(t) = \hat{\alpha}$ and the set-up function $\epsilon^2 \hat{\Upsilon}(t, T, \mathbf{p}^*)$ are depicted in the real time coordinate $t \in [0, T]$. Obviously, $\hat{\alpha}$ in (19) is “re-planned” twice, i.e. $\ddot{y}^*(t) \neq \epsilon^2 \hat{\Upsilon}(t, T, \mathbf{p}^*)$, such that the feedforward control (12) meets the input constraints \hat{u} . In these cases, the feedforward trajectory $u^*(t)$ in Figure 3 stays constant at ± 0.7 Nm.

³ In (Graichen *et al.*, 2004a; Graichen *et al.*, 2004b), the output trajectory $y^*(t)$ is set-up with polynomials in a slightly different way. For complex transition problems like the swing-up maneuver of the pendubot, cosine series are numerically more robust.

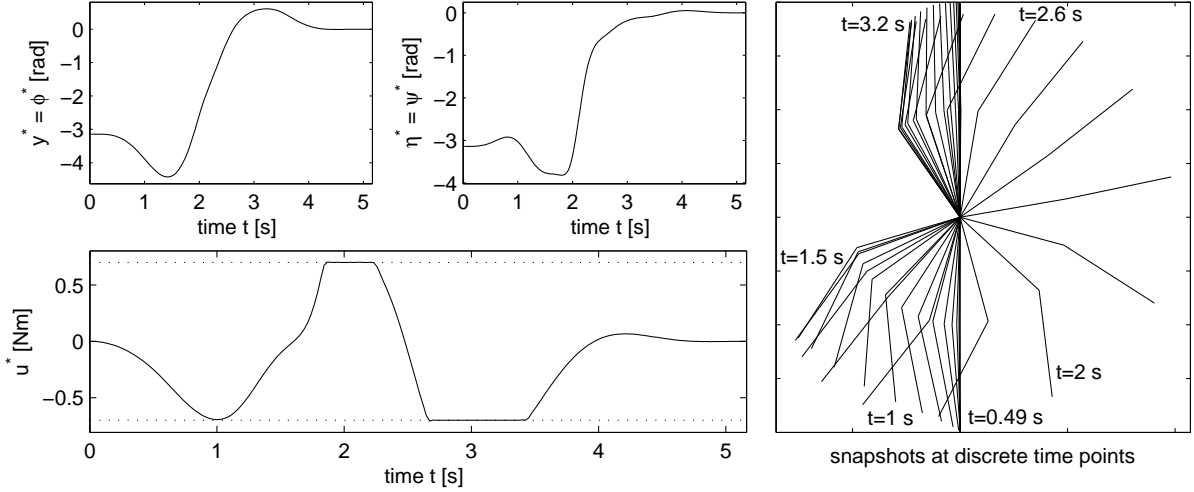


Fig. 3. Nominal feedforward trajectories $y^*(t) = \phi^*(t)$, $\eta^*(t) = \psi^*(t)$, and $|u^*(t)| \leq 0.7 \text{ Nm}$, as well as time-discrete snapshots for the swing-up maneuver with $T = 5.16 \text{ s}$, and $\mathbf{p}^* = (0.305, -0.178, -0.106)$, $a_1 = -2.123$, $a_2 = -0.268$, $a_3 = 0.730$ in (18) and (19).

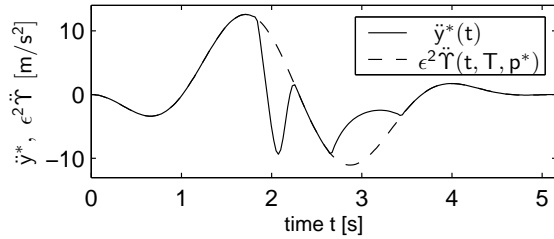


Fig. 4. Second derivative $\ddot{y}^*(t) = \hat{\alpha}$ of the output and set-up function $\epsilon^2 \tilde{\ddot{\Upsilon}}(t, T, \mathbf{p}^*)$ for the swing-up maneuver.

4. FEEDBACK CONTROL DESIGN AND EXPERIMENTAL RESULTS

The experimental validation of the feedforward control for the swing-up maneuver requires a stabilization by feedback Σ_{FB} , see Figure 1. Due to the high accuracy of the nonlinear feedforward control Σ_{FF} , the feedback part Σ_{FB} can be designed by linear methods with the pendubot model linearized along the nominal trajectories, such that

$$u = u^* + \mathbf{k}^T(t)(\mathbf{x}^* - \mathbf{x}) \quad (20)$$

is the input in closed-loop control. The time-variant vector $\mathbf{k}^T(t)$ with the gains $k_i(t)$, $i = 1, 2, 3, 4$ of the states $\mathbf{x} = (\phi, \dot{\phi}, \psi, \dot{\psi})$ are calculated point-wise in time by an LQR technique with weighting matrices $Q = \text{diag}(1, 0, 2, 0)$ and $R = 5/(\text{Nm})^2$. Thereby, it must be considered that the controllability of the linearized model is lost in the mid of the swing-up maneuver at approximately $t = 2.6 \text{ s}$, which leads to a finite-time blow-up of the controller gains $k_i(t)$. This problem is avoided by interpolating the feedback gains $k_i(t)$ through the singularity during the time interval $t \in [2.4, 2.8] \text{ s}$, see Figure 5, as well as Figure 3 for the respective positions of the pendubot arms at $t = 2.6 \text{ s}$.

The tracking control has been validated in experimental swing-up maneuvers of the pendubot with mechanical parameters given in Table 1. The angles ϕ and ψ are measured by two optical sensors with a resolution of 250 points/ π . The time derivatives $\dot{\phi}$ and $\dot{\psi}$ required by the feedback control are determined by a numerical difference scheme. The designed feedforward and feedback controls have been implemented in LabVIEW on a PC Pentium II/300 with a sampling time of 10 ms. The nominal state trajectories $\phi^*(t)$, $\dot{\phi}^*(t)$, $\psi^*(t)$, $\dot{\psi}^*(t)$, the feedforward control $u^*(t)$, and the time-variant feedback gain vectors $k_i(t)$, $i = 1, 2, 3, 4$ are stored in look-up tables with 200 elements for the swing-up maneuver of the pendubot.

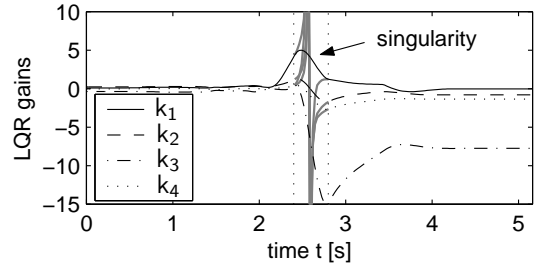


Fig. 5. Time-variant LQR feedback gains $k_i(t)$ with interpolation through the singularity.

Figure 6 shows the experimental and nominal trajectories of the angles $y = \phi$ and $\eta = \psi$ and the input u for open-loop and closed-loop control of the swing-up maneuver. The open-loop trajectories reveal the good accuracy of the designed feedforward control $u^*(t)$, but the pendubot drifts away from the unstable upward position. In closed-loop, the feedback control stabilizes the pendubot along the nominal trajectories $y^*(t) = \phi^*(t)$ and $\eta^*(t) = \psi^*(t)$ and also in the unstable upward position. The noise in the input trajectory $u(t)$ for $t > 2.5 \text{ s}$ is mainly due to the numerical differentiation of ϕ and ψ and

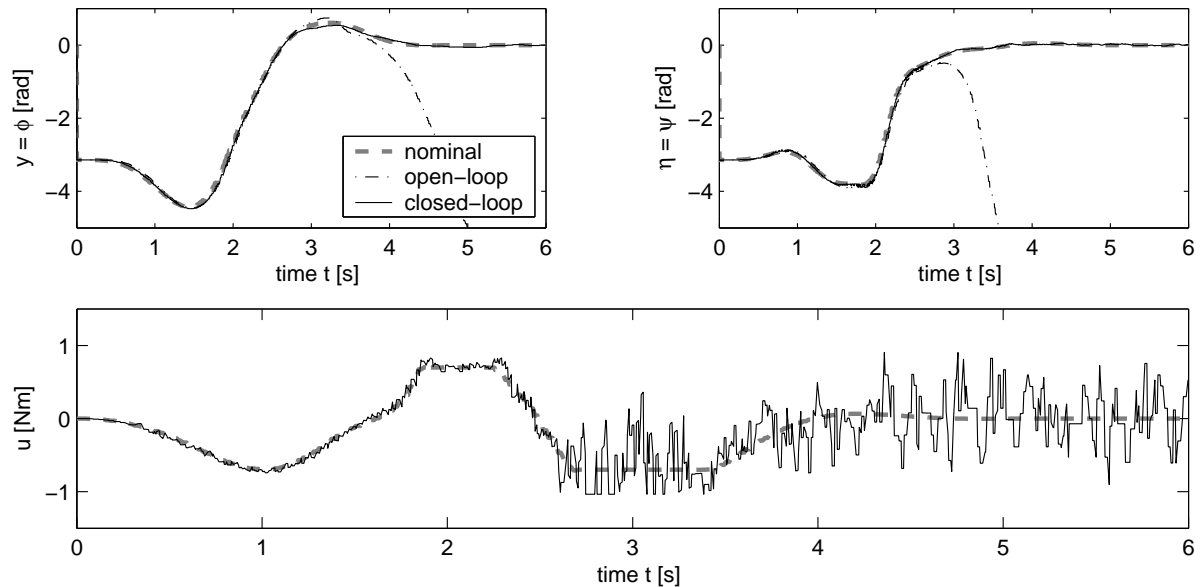


Fig. 6. Experimental and nominal trajectories of the angles ϕ , ψ , and the input u for the tracking control of the pendubot swing-up maneuver with $T = 5.16$ s, $|u^*(t)| \leq 0.7$ Nm, and the model parameters in Table 1.

the low resolution of the optical sensors, as well as due to the high amplitudes of the feedback gains $k_i(t)$ in the upward unstable position of the pendubot, see Figure 5. The comparison between the nominal and experimental trajectories reveals very good tracking performance such that the designed tracking control allows reproducible swing-up maneuvers of the pendubot.⁴

5. CONCLUSIONS

The presented design approach of nonlinear feedforward control solves the swing-up problem of the pendubot as a two-point BVP with free parameters by additionally considering input constraints of the actuator. In the unconstrained case, this approach is equivalent to the inversion-based feedforward control design technique proposed by the authors (Graichen *et al.*, 2004a; Graichen *et al.*, 2004b). Open questions of the applied two-degree-of-freedom control scheme with a nonlinear feedforward and a linear feedback part concern the existence and uniqueness of solutions to the BVP with input constraints in course of the feedforward design for the swing-up maneuver and a theoretical analysis of the robust stabilization by the time-variant feedback gains.

ACKNOWLEDGEMENTS

The authors gratefully acknowledge the support of Dr. Hanss and Dr. Steinwand with the provision and the experimental setup of the pendubot at the Institut A für Mechanik at Universität Stuttgart.

⁴ In the student thesis of Christian Bermes (2005), the finite-time transition between all four equilibrium points of the pendubot are studied and realized in the experiment.

REFERENCES

- Absil, P.-A. and R. Sepulchre (2001). A hybrid control scheme for swing-up acrobatics. In: *Proc. 6th Europ. Contr. Conf.*. pp. 2860–2864.
- Block, D.J. and M.W. Spong (1995). Mechanical design and control of the pendubot. In: *46th SAE Earthmoving Indus. Conf.*
- Fantoni, I., R. Lozano and M.W. Spong (2000). Energy based control of the pendubot. *IEEE Trans. Automat. Contr.* **45**, 725–729.
- Graichen, K., V. Hagenmeyer and M. Zeitz (2004a). A new approach to inversion-based feedforward control design for nonlinear systems (submitted).
- Graichen, K., V. Hagenmeyer and M. Zeitz (2004b). Van de Vusse CSTR as a benchmark problem for nonlinear feedforward control design techniques. *6th IFAC-Symp. Nonl. Contr. Syst.*, Stuttgart (Germany).
- Isidori, A. (1995). *Nonlinear Control Systems*. 3rd ed.. Springer.
- Murray, R. and J. Hauser (1990). A case study in approximate linearization: The acrobot example. *Proc. Amer. Contr. Conf.* cite-seer.ist.psu.edu/murray90case.html.
- Shampine, L.F., J. Kierzenka and M.W. Reichelt (2000). Solving boundary value problems for ordinary differential equations in MATLAB with `bvp4c`.
<ftp://ftp.mathworks.com/pub/doc/papers/bvp/>.
- Spong, M.W. (1995). The swing up problem for the acrobot. *IEEE Contr. Syst. Mag.* **15**, 49–55.
- Spong, M.W. and D.J. Block (1995). The pendubot: A mechatronic system for control research and education. In: *Proc. 34th IEEE Conf. Dec. Contr.*. pp. 555–556.